

## EXPRESS LETTER

# A new unified approach to determine geocentre motion using space geodetic and GRACE gravity data

Xiaoping Wu<sup>1</sup>, Jürgen Kusche<sup>2</sup> and Felix W. Landerer<sup>1</sup>

<sup>1</sup>*Jet Propulsion Laboratory, California Institute of Technology, Pasadena, CA 91109, USA. E-mail: Xiaoping.Wu@jpl.nasa.gov*

<sup>2</sup>*Institute of Geodesy and Geoinformation, University of Bonn, D-53115 Bonn, Germany*

Accepted 2017 March 2. Received 2017 February 26; in original form 2016 December 6

## SUMMARY

Geocentre motion between the centre-of-mass of the Earth system and the centre-of-figure of the solid Earth surface is a critical signature of degree-1 components of global surface mass transport process that includes sea level rise, ice mass imbalance and continental-scale hydrological change. To complement GRACE data for complete-spectrum mass transport monitoring, geocentre motion needs to be measured accurately. However, current methods of geodetic translational approach and global inversions of various combinations of geodetic deformation, simulated ocean bottom pressure and GRACE data contain substantial biases and systematic errors. Here, we demonstrate a new and more reliable unified approach to geocentre motion determination using a recently formed satellite laser ranging based geocentric displacement time-series of an expanded geodetic network of all four space geodetic techniques and GRACE gravity data. The unified approach exploits both translational and deformational signatures of the displacement data, while the addition of GRACE's near global coverage significantly reduces biases found in the translational approach and spectral aliasing errors in the inversion.

**Key words:** Global change from geodesy; Loading of the Earth; Satellite geodesy; Time variable gravity.

## 1 INTRODUCTION

Assuming mass conservation in the Earth's surface fluid layer, spherical harmonic expansions of global surface mass variations start from three degree-1 terms. These longest wavelength variations drive and are proportional to geocentre motion between the centre-of-mass of the Earth system (CM) and the centre-of-figure (CF) of the solid Earth surface. By choosing CM as the coordinate origin, the Gravity Recovery and Climate Experiment (GRACE) data system contains no degree-1 gravity coefficients. More importantly, GRACE's K-band ranging data are not sensitive to the degree-1 surface mass variation coefficients or geocentre motion. As critical parts of the complete mass variation spectra and regional mass budgets, the missing degree-1 surface mass coefficients need to be measured independently and accurately with reliable assessment of uncertainties to supplement GRACE data (see Wu *et al.* 2012 for a review). Also, since geodetic satellites orbit around CM and are tracked by stations on the Earth's surface, geocentre motion has significant implications on consistent and accurate orbit determinations and ocean tide measurements (Beckley *et al.* 2007; Desai & Ray 2014).

One method for geocentre motion estimation is a translational or network shift approach that seeks to determine mean geocen-

tic displacement time-series from a network of satellite tracking ground stations. In most cases, estimations are carried out by stacking coordinate time-series against linear motion models such as International Terrestrial Reference Frame (ITRF) solutions. The result is thus (after a sign change) equivalent to nonlinear CM motion with respect to the centre-of-(tracking) network (CN), which is used to approximate CM-CF motion. The method can theoretically work for any satellite tracking technique with ground stations fixed on the surface, and has been applied to Satellite Laser Ranging (SLR), Global Navigation Satellite System (GNSS) and Doppler Orbitography and Radio Positioning Integrated by Satellites (DORIS). The DORIS system has relatively higher noises in tracking data and annual geocentre motion results with satellite specific errors (e.g. Bouille *et al.* 2000; see also, e.g. Moreaux *et al.* 2016 for recent improvements). Despite recent progress, GNSS may contain inherent data weaknesses due to simultaneous estimation of clock and tropospheric parameters (e.g. Rebischung *et al.* 2014; Kuang *et al.* 2015) and sizable 'draconitic' errors arising from mismodelled solar radiation pressure (Meindl *et al.* 2013; Haines *et al.* 2015). Consequently, annual translational geocentre motion determinations, including the method of tracking low Earth orbiters, remain challenging for GNSS. SLR appears to have the most reliable sensitivity to CM due to simpler orbit dynamics and has

offered the first competitive geocentre motion result (Eanes *et al.* 1997; Bouille *et al.* 2000; Cheng *et al.* 2013; Glaser *et al.* 2015). However, SLR ground stations are very sparse and unevenly distributed with about 20 active stations on average, with significant turnovers in recent years and only a dozen or so stations supplying the bulk of tracking data. Such a CM-CN motion, and similarly, CM-CN motions obtained from many other geodetic networks may be significantly different from CM-CF motion required to complement GRACE data. The approximation error depends on station distribution and surface mass variation scenario and can reach the level of 1–2 mm in annual amplitude (Wu *et al.* 2012). Recently, the SLR-based geocentric network has been extended to contain 82 better-distributed stations including those from other geodetic techniques through local tie measurements and co-motion constraints when an experimental Kalman filter and time-series terrestrial reference frame realization was carried out (Wu *et al.* 2015). Although the CM-CN motion of the expanded network should better approximate CM-CF motion, there is no guarantee that the two motions are close enough without knowing the exact approximation error.

Another type of method is to invert for degree-1 surface mass variation coefficients from various combinations of relative deformation of GNSS stations, ocean bottom pressure models, Jason ocean altimetry, and GRACE data (Blewitt & Clarke 2003; Wu *et al.* 2006; Swenson *et al.* 2008; Rietbroek *et al.* 2016). In many cases, higher degree coefficients have also been estimated simultaneously or derived from GRACE data. GNSS stations are unevenly distributed geographically with sparse coverage in oceanic areas and the Southern Hemisphere. The degree-1 deformational signatures are also much weaker than those of the translational geocentre motion, with the extent strongly depending on site distribution. The addition of an ocean bottom pressure model and GRACE data apparently improves geographic coverage and the separation of spherical harmonic coefficients. However, ocean bottom pressure models generally do not conserve mass or contain accurate mass input/output information (i.e. from evaporation, precipitation, and discharge). They are also built on the static geoid without considering time-variable self-gravitation and loading effects of surface mass variations. While these problems can be, and have been corrected (e.g. Sun *et al.* 2016), a more serious concern is that ocean circulation models, even if many oceanographic data may be assimilated, perhaps remain poorly skilled in reproducing ocean bottom pressure. The unknown model errors on the small oceanic contribution to geocentre motion will directly affect global inversion results, and result in amplified errors in full geocentre motion if only GRACE and ocean models are combined.

A unified approach using both translational and deformational signatures of degree-1 surface mass variations in the GNSS data has been proposed, which also estimates a zonal degree-2 coefficient (Lavallée *et al.* 2006). Aside from erroneous GNSS translational signals along the  $z$ -axis mentioned above, the truncation at C20 appears too severe to effectively remove aliasing errors from neglected higher-degree coefficients.

In this paper, we take a new unified approach to geocentre motion determination by combining the geocentric coordinate time-series of the 82-station network with GRACE gravity data. The translational signal in this case is based on SLR and thus not subject to the direct impact of GNSS translational errors. Both translational and deformational signatures of the displacement time-series are consistently modelled and explored in the observation equations as functions of estimated surface mass variation coefficients from degree-1 to degree-43. The addition of the GRACE data will significantly improve the CN-CF approximation and enhance the separation of

degree-1 coefficients from those of other spherical harmonic terms. Full variance-covariance matrices of all data are used. For estimate objectivity and optimal assessment of the estimate uncertainties, a variance component estimation (VCE) procedure is also carried out. The new method and data combination will be described in the next section. The results will be presented in Section 3 followed by discussion and conclusions.

## 2 METHODS AND DATA

The nonlinear load-induced geocentric displacement at site  $i(\vartheta, \varphi)$  in the centre-of-mass of the solid Earth (CE) frame (or any other frame) against a reference epoch can be written as (Farrell 1972):

$$\mathbf{s}_i^g = \mathbf{s}_i - \mathbf{s}_{cm} = \frac{4\pi a^3}{M_E} \sum_{n=1}^{\infty} \sum_{m=0}^n \sum_{q=c,s} \frac{M_{nmq}}{2n+1} \\ \times \left[ h'_n Y_{nmq} \hat{\mathbf{e}}_r + l'_n \partial_{\vartheta} Y_{nmq} \hat{\mathbf{e}}_{\vartheta} + l'_n \frac{1}{\sin \vartheta} \partial_{\varphi} Y_{nmq} \hat{\mathbf{e}}_{\varphi} \right] - \mathbf{s}_{cm}, \quad (1)$$

where  $\mathbf{s}_i$  and  $\mathbf{s}_{cm}$  are displacements of the site and CM respectively,  $a$  is the mean Earth radius,  $M_E$  the Earth's mass,  $h'_n$  and  $l'_n$  the vertical and horizontal load Love numbers respectively in the corresponding frame (CE in this case),  $M_{nmq}$  is the spherical harmonic coefficient of surface mass density change, and  $Y_{nmq}(\vartheta, \varphi)$  the spherical harmonic function. In the CE frame,  $\mathbf{s}_{cm}$  is a function of  $M_{1mq}$ :

$$\mathbf{s}_{cm} = \frac{4\pi a^3}{\sqrt{3} M_E} (M_{11c} \hat{\mathbf{e}}_x + M_{11s} \hat{\mathbf{e}}_y + M_{10c} \hat{\mathbf{e}}_z), \quad (2)$$

and when eq. (1) is integrally averaged on the surface of the solid Earth with a change of sign, geocentre motion is then derived between CM and CF (Trupin *et al.* 1992):

$$\mathbf{s}_{cm} - \mathbf{s}_{cf} = \frac{4\pi a^3}{\sqrt{3} M_E} \left( 1 - \frac{h'_1 + 2l'_1}{3} \right) \\ \times (M_{11c} \hat{\mathbf{e}}_x + M_{11s} \hat{\mathbf{e}}_y + M_{10c} \hat{\mathbf{e}}_z). \quad (3)$$

Eqs (2) and (3) are very similar since  $\mathbf{s}_{cf}$  is only about 2 per cent of  $\mathbf{s}_{cm}$  (Dong *et al.* 1997). But geocentre motion is preferably defined by the latter because it is theoretically accessible by satellite geodetic techniques and the components have one-to-one correspondences with the three degree-1 coefficients.

The network shift approach is equivalent to take a negative mean geocentric displacement of all the sites in the network as  $\mathbf{s}_{cm} - \sum_{i=1}^N \mathbf{s}_i / N$ , which is identical to the motion between CM and CN. Although the approach itself does not involve spherical harmonics, the derived CM-CN motion has been used to approximate CM-CF and thus degree-1 coefficients through eq. (3). The derived mean displacement can be further expressed in spherical harmonic domain using eq. (1). Because the sites cannot be globally dense, the higher degree ( $n > 1$ ) terms will not cancel out in the average displacement, and the discrete sum of degree-1 terms are not the same as their integral. Consequently, the CM-CN motion will usually be different from CM-CF. The unified approach uses degree-1 signatures in both (deformational and translational) terms of the right-hand side of eq. (1) after replacing  $\mathbf{s}_{cm}$  with eq. (2). But the successful retrieval of  $M_{1mq}$  depends on the magnitudes of the higher degree terms in the equation, and on how well these can be separated from the degree-1 terms.

The geocentric displacement time-series for this study resulted from a recent Kalman filter and time-series realization of terrestrial reference frame by combining coordinate time-series of all four

space geodetic techniques (see Wu *et al.* 2015 for details). The nearly instantaneous CM as observed by SLR is chosen to realize the coordinate origin. The intrinsic weighted average scales of SLR and VLBI are used for the nearly instantaneous frame scale. Networks of other geodetic techniques are tied to the geocentric frame through local tie measurements and co-motion constraints between co-located stations. The orientation of the frame is defined by no-net-rotation constraints to a linear predecessor frame which itself is defined by convention and a no-net-rotation plate motion model (Altamimi *et al.* 2011). The motion model consists of linear and seasonal components, as well as a stochastic component that is a white noise driven random walk with site specific but constant *a priori* variances based on a load-induced deformation model. The result of Kalman filter and smoother operation is weekly coordinate time-series at 580 sites including all four techniques from 1980.0 to 2009.5 with full covariance matrices. A sub-network of 82 sites with more uniform distribution and dense data is then chosen for this study. One consequence of the normal sequential filter/smooth operation, however, is that the errors in the weekly coordinate solutions are correlated in time, but the correlations are not retained.

Starting from March of 2002, the GRACE mission has been observing time-variable gravity on a near monthly basis. For non-linear variations, the changing geoid coefficients are proportional to surface mass density change coefficients (Wahr *et al.* 1998):

$$N_{nmq} = \frac{4\pi a^3}{M_E} \frac{1+k'_n}{2n+1} M_{nmq}, \quad n = 2, n_{\max}. \quad (4)$$

These measurements apparently can help separating higher ( $n > 1$ ) degree-terms in eq. (1). For this study, we use the official RL05 data from Center for Space Research, the University of Texas at Austin, with monthly mean atmospheric and oceanic dealiasing products restored, and empirically calibrated full covariance matrices. GRACE's C20 time-series has been replaced by that determined from SLR.

In our new unified approach, we substitute eq. (2) into eq. (1) and combine the geocentric displacements data with GRACE geoid coefficients in eq. (4) to estimate  $M_{nmq}$  from 2002.2 to 2009.0 when both SLR input time-series to KALREF and GRACE data are available. To filter out increasing data noise in higher degree GRACE data, the estimation also uses an *a priori* parameter model with zero mean values and a temporally constant diagonal covariance matrix derived from root mean square variations predicted by a geophysical model of combined atmospheric, oceanic and hydrological loading. To be compatible with the gravity data, the weekly geocentric displacements and their covariance matrices are averaged into quasi-monthly periods of the GRACE data. Since the temporal correlations are ignored, the resulting average covariance matrices may be significantly underestimated. Both data sets are then referenced against a common epoch with linear trends removed. Although the GRACE covariance matrices are deemed fairly reliable, a preliminary estimation shows an increasing number of large residuals ( $>3\sigma$ ) above degree 43. We therefore decided to truncate the GRACE data further at degree 43. To increase reliability of the estimation, an iterative Helmert variance component estimation process is also undertaken (Koch & Kusche 2002) to determine quasi-monthly root variance factors for the displacement and GRACE data as well as the *a priori* model. Finally, the parameter estimation is carried out using the least squares method with reduced *a priori* information. Under the platform of singular value decomposition, the method discards *a priori* information if it is noisier than the data (Wu *et al.* 2006). To further reduce reliance on the

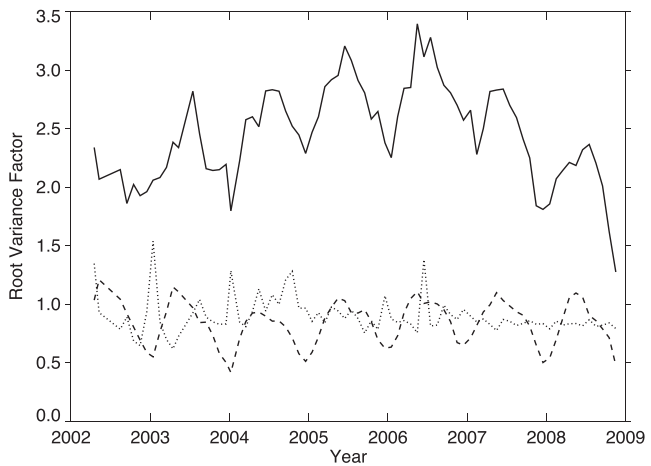


**Figure 1.** Quasi-monthly root variance factors for displacements (solid line), GRACE gravity data (dotted line) and *a priori* geophysical model (dashed line) resulted from the variance component estimation procedure.

model prediction, the *a priori* variances are enlarged by a factor of 4, and the *a priori* variances for lower degree ( $\leq 25$ ) parameters are further enlarged by a factor of  $10^6$ . However, these adjustments of truncation degree and *a priori* variances do not affect the inversion significantly, with impact on geocentre motion generally  $<0.1$  mm in annual amplitudes.

### 3 RESULTS

The Helmert VCE generally converges to the level of  $10^{-3}$  after a few iterations. Fig. 1 shows the root variance results, which, after squared, are scaling factors for the nominal covariance matrices. The larger displacement root variance factors show that the nominal average monthly displacement covariance matrices are significantly underestimated perhaps due to the neglect of temporal correlations, effects not induced by loading, and unaccounted-for systematic measurement errors. The RMS posteriori root variance factor for monthly displacements is about 2.2. In addition, an apparent seasonal behaviour can be seen in the temporal curve. The displacement data used in the inversion are detrended and weighted monthly average coordinate differences against a reference month using the KALREF estimated weekly coordinate states including linear, seasonal, and stochastic components. It is conceivable that the ignored correlations might have contributed to the seasonal variance pattern. To investigate this possibility, KALREF coordinate estimates using very large (5 cm) *a priori* root variance for the stochastic component are used with GRACE in a test inversion with VCE. The large stochastic component dramatically decreases the significance of linear and seasonal component estimation, and reduces temporal correlations in the state estimates. The seasonality then disappears in the root variance factor time-series for the test displacement data. The root variance factors for the *a priori* model also show a strong seasonality with an RMS value of 1.05. Because a constant formal *a priori* covariance matrix is used for all GRACE quasi-months, and the changes referenced against a particular month should have an annual cycle, the seasonal behaviour in the root variance factor is actually expected. In contrast, no seasonality is found in the root variance factors for the largely independent quasi-monthly GRACE data. Apart from a few months, the nominal calibrated GRACE data covariance matrices are only slightly overestimated. These results indicate to us that the Helmert VCE procedure is rather successful.

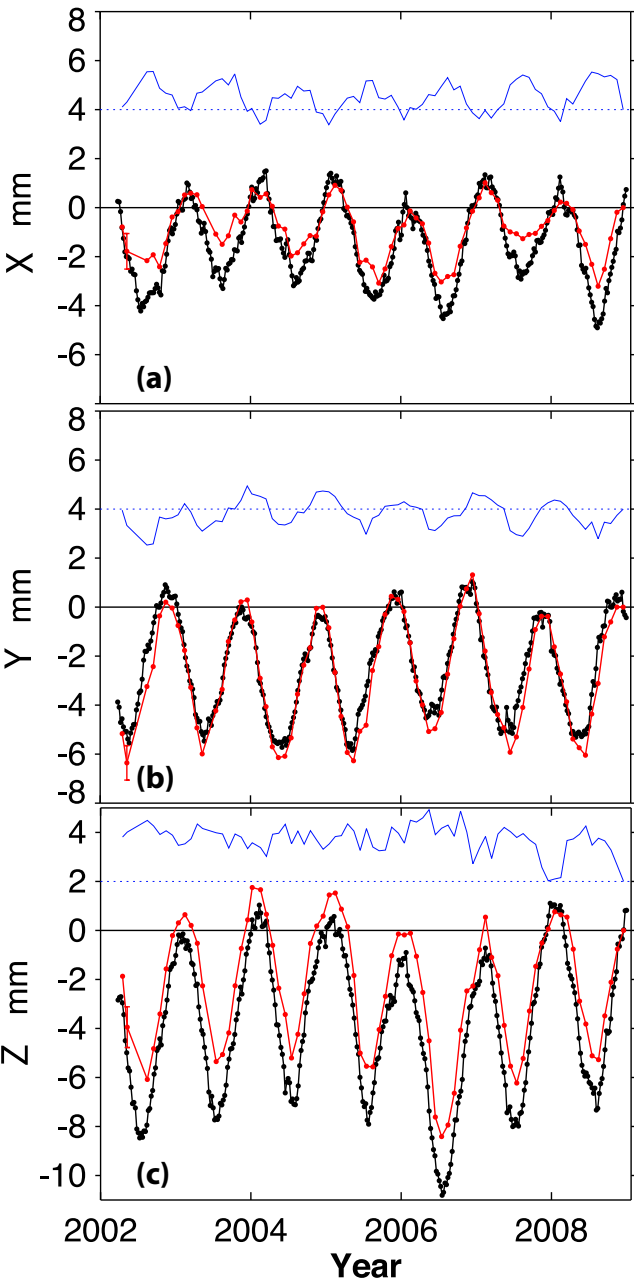


**Figure 2.** KALREF determined weekly CM-CN motion using an 82-station network (black linked dots) compared with estimated quasi-monthly CM-CF motion using geocentric displacements of the 82-station and GRACE gravity data (linked red dots). The three panels (a–c) show  $X$ ,  $Y$  and  $Z$  components respectively. Blue lines in the panels show quasi-monthly differences of the two types of motion components (red-black) or equivalently, CN-CF, and have been shifted by 4, 4, and 2 mm for the  $XYZ$  components respectively for better demonstrations.

Fig. 2 shows the inverted geocentre motion (CM-CF) time-series along with the 82-station CM-CN result reported earlier in Wu *et al.* (2015). For all three components, the two time-series correlate quite well in time. For  $Y$ , the curves are also very similar. The fitted annual amplitudes and phases are listed in Table 1. The posteriori unit weight uncertainties for the least squares fits are 0.84, 0.75 and 1.20 respectively, for the  $X$ ,  $Y$  and  $Z$  components. These further indicate that the VCE and the 6-parameter fit are quite successful. The estimated parameter uncertainties are also listed in Table 1 with

that of the  $Z$ -component upscaled by 1.20 to result in a larger uncertainty than those of  $X$  and  $Y$  components. The VCE and post-fit uncertainty scaling procedures both serve to reduce the effect of omitting temporal correlations in the inversion and post-inversion temporal fit. However, the final uncertainty estimates may still be slightly underestimated due to the remaining effect of correlation omission and other factors.

For the  $X$  component, however, the inverted geocentre motion amplitude is persistently smaller than that of the CM-CN result derived from the network shift approach as can be clearly seen from Fig. 2 and Table 1. The  $Z$  component of CM-CF also has a smaller annual amplitude and a negative shift compared to that of CM-CN. On the other hand, the annual phases do not seem to change significantly. This further reinforces the notion that although the 82-site CM-CN can better approximate CM-CF than the sparse operating SLR network, it is still fundamentally different from CM-CF, and the 0.7 mm approximation error, which corresponds to an annual mean sea level error of 0.35 mm, is too large to be ignored. As a consequence of consistent combination of the displacement and gravity data, the annual amplitude of  $X$  component of CM-CF in our study is also significantly smaller than those estimated in previous inversion studies. The new unified data approach should be considered more reliable due to its signature strength and global spatial coverage without the adverse effect of depending on ocean models used in previous inversions. We also note that the formal uncertainties quoted in previous studies usually do not reflect systematic or spatiotemporally correlated errors in data and ocean models.

#### 4 DISCUSSION AND CONCLUSIONS

The degree-1 coefficients to be combined with GRACE gravity data for full spectrum surface mass variation monitoring requires accurate knowledge of geocentre motion between CM and CF, with accuracy goals of 0.2 mm for annual amplitude and 0.2 mm  $\text{yr}^{-1}$  for velocity. Depending on mass variation scenarios and network distributions, CM-CN motion can be quite different from that of CM-CF. This significantly limits the accuracy in using CM-CN motion to approximate that of CM-CF and, subsequently, the degree-1 surface mass variation coefficients.

Our new unified method is mostly based on space geodetic and GRACE gravity data, with very little dependence on the *a priori* geophysical model. The inversion for geocentre motion appears to work quite well, especially along  $X$ - and  $Y$ -axes. However, along the  $Z$ -axis, evidences of moderate temporally correlated errors and inconsistencies between site displacement and spherical harmonic gravity data can be seen in estimation residuals. Possible reasons for these are remaining draconitic errors in reprocessed GNSS data, inaccurate or neglected intrinsic variance and correlation structures in covariance matrices, unaccounted-for systematic errors, and truncated higher-degree terms, in addition to time-correlated errors in KALREF displacements discussed before. The impacts of these factors on parameter estimation, for the most part, are not precisely known, but may be limited as suggested by a very good agreement (within  $1.4\sigma$ ) between the independent SLR C20 measurements and our inverted C20 results without using GRACE or SLR C20 data. The SLR C20 data and inversion results show respective annual amplitudes of  $(14.4 \pm 0.9) \times 10^{-11}$  and  $(15.0 \pm 1.2) \times 10^{-11}$ , with respective peak times at  $57 \pm 3$  and  $49 \pm 5$  day. Consequently, the true uncertainties of our annual geocentre motion estimates along the  $Z$ -axis may only be slightly higher (at  $\pm 0.3$  mm in annual amplitude) than those listed in Table 1.

**Table 1.** Comparison of annual geocentre motion estimates approximately during 2002.2–2009.0.

Method and data	$X_g$		$Y_g$		$Z_g$		Ref.
	Amp. (mm)	Phase (day)	Amp. (mm)	Phase (day)	Amp. (mm)	Phase (day)	
SLR-Monthly 20+ site CM-CN	$2.9 \pm 0.4$	$36 \pm 3$	$2.6 \pm 0.2$	$310 \pm 2$	$4.2 \pm 0.3$	$33 \pm 2$	Cheng <i>et al.</i> (2013)
GNSS Unified 1997.2–2004.2 CM-CF	$2.1 \pm 0.2$	$39 \pm 4$	$3.2 \pm 0.1$	$346 \pm 2$	$3.9 \pm 0.2$	$74 \pm 2$	Lavallée <i>et al.</i> (2006)
GNSS+GRACE+OBP CM-CF	$1.8 \pm 0.1$	$49 \pm 4$	$2.7 \pm 0.1$	$329 \pm 2$	$4.2 \pm 0.2$	$31 \pm 3$	Wu <i>et al.</i> (2012)
Jason 1/2 Alt.+GRACE CM-CF	$2.2 \pm 0.2$	$54 \pm 4$	$2.7 \pm 0.2$	$333 \pm 4$	$3.5 \pm 0.4$	$62 \pm 5$	Rietbroek <i>et al.</i> (2016)
OBP+GRACE 2002.6–2014.5 CM-CF	$2.3 \pm 0.1$	$52 \pm 3$	$2.8 \pm 0.1$	$327 \pm 2$	$2.9 \pm 0.2$	$69 \pm 4$	Sun <i>et al.</i> (2016)
KALREF-week 82-site CM-CN	$2.1 \pm 0.1^a$	$45 \pm 1$	$2.7 \pm 0.1$	$321 \pm 1$	$3.8 \pm 0.1$	$21 \pm 1$	Wu <i>et al.</i> (2015)
KALREF-month <sup>b</sup> 82-site CM-CN	$2.0 \pm 0.1^a$	$45 \pm 3$	$2.7 \pm 0.1$	$319 \pm 2$	$3.7 \pm 0.2$	$22 \pm 3$	Wu <i>et al.</i> (2015)
KALREF+GRACE <sup>b</sup> CM-CF	$1.3 \pm 0.1$	$46 \pm 4$	$3.0 \pm 0.1$	$330 \pm 2$	$3.3 \pm 0.2$	$26 \pm 3$	This study

<sup>a</sup>All KALREF formal uncertainties may be significantly underestimated without time-correlated information.

<sup>b</sup>Averaged over quasi-monthly GRACE periods. The weekly time-series have slightly larger annual amplitudes. The phases correspond to peak times.

Although we only focus on nonlinear geocentre motion here to avoid complications and uncertainties of the glacial isostatic adjustment (GIA) process, the method in principle can be extended to linear geocentre motion in the future when GIA is modelled or estimated and when linear reference frame origin stability is better understood and improved.

## ACKNOWLEDGEMENTS

This work was carried out at the Jet Propulsion Laboratory, California Institute of Technology, under a contract with the National Aeronautics and Space Administration (NASA), and funded through NASA's GRACE Science Team, MEaSUREs, and Interdisciplinary Research in Earth Science programs. GRACE level-2 data are publicly available from <http://podaac.jpl.nasa.gov/grace/>. SLR C20 time-series and calibrated GRACE data covariance matrices are from Minkang Cheng and John Ries respectively. Geocentric displacement time-series were described in Wu *et al.* (2015) and are available through the ITRF website.

## REFERENCES

- Altamimi, Z., Collilieux, X. & Métivier, L., 2011. ITRF2008: an improved solution of the international terrestrial reference frame, *J. Geod.*, **85**(8), 457–473.
- Beckley, B. D., Lemoine, F.G., Luthcke, S.B., Ray, R.D. & Zelensky, N.P., 2007. A reassessment of global and regional mean sea level trends from TOPEX and Jason-1 altimetry based on revised reference frame and orbits, *Geophys. Res. Lett.*, **34**, L14608, doi:10.1029/2007GL030002.
- Blewitt, G. & Clarke, P., 2003. Inversion of Earth's changing shape to weigh sea level in static equilibrium with surface mass redistribution, *J. geophys. Res.*, **108** (B6), 2311, doi:10.1029/2002JB002290.
- Bouille, F., Cazenave, A., Lemoine, J.M. & Creteaux, J.F., 2000. Geocenter motion from the DORIS space system and laser data on Lageos satellites: comparison with surface loading data, *Geophys. J. Int.*, **143**, 71–82.
- Cheng, M.K., Ries, J.C. & Tapley, B.D., 2013. Geocenter motion from analysis of SLR Data, in *International Association of Geodesy Symposia*, vol. 138, pp. 19–25, eds Altamimi, Z. & Collilieux, X., Springer-Verlag.
- Desai, S.D. & Ray, R.D., 2014. Consideration of tidal variations in the geocenter on satellite altimeter observations of ocean tides, *Geophys. Res. Lett.*, **41**, 2454–2459.
- Dong, D., Dickey, J.O., Chao, Y. & Cheng, M.K., 1997. Geocenter variations caused by atmosphere, ocean and surface ground water, *Geophys. Res. Lett.*, **24**, 1867–1870.
- Eanes, R.J., Kar, S., Bettadapur, S.V. & Watkins, M.M., 1997. Low-frequency geocenter motion determined from SLR tracking (abstract), *EOS, Trans. Am. geophys. Un.*, **78**(46), Fall Meet. Suppl., F146.
- Farrell, W.E., 1972. Deformation of the Earth by surface loads, *Rev. Geophys.*, **10**, 761–797.
- Glaser, S. *et al.*, 2015. A consistent combination of GNSS and SLR with minimum constraints, *J. Geod.*, **89**, 1165–1180.
- Haines, B.J., Bar-Sever, Y.E., Bertiger, W.I., Desai, S.D., Harvey, N., Sibois, A.E. & Weiss, J.P., 2015. Realizing a terrestrial reference frame using the Global Positioning System, *J. geophys. Res.*, **120**, 5911–5939.
- Koch, K.-R. & Kusche, J., 2002. Regularization of geopotential determination from satellite data by variance components, *J. Geod.*, **76**, 259–268.
- Kuang, D., Bar-Sever, Y. & Haines, B., 2015. Analysis of orbital configurations for geocenter determination with GPS and low-Earth orbiters, *J. Geod.*, **89**(5), 471–481.
- Lavallée, D.A., van Dam, T., Blewitt, G. & Clarke, P.J., 2006. Geocenter motions from GPS: a unified observation model, *J. geophys. Res.*, **111**(B5), B05405, doi:10.1029/2005JB003784.
- Meindl, M., Beutler, G., Thaller, D., Dach, R. & Jaggi, A., 2013. Geocenter coordinates estimated from GNSS data as viewed by perturbation theory, *Adv. Space Res.*, **51**(7), 1047–1064.
- Moreaux, G., Lemoine, F.G., Capdeville, H., Kuzin, S., Otten, M., Štěpánek, P., Willis, P. & Ferrage, P., 2016. The International DORIS Service contribution to the 2014 realization of the International Terrestrial Reference Frame, *Adv. Space Res.*, **58**(12), 2479–2504.
- Rebischung, P., Altamimi, Z. & Springer, T., 2014. A collinearity diagnosis of the GNSS geocenter determination, *J. Geod.*, **88**, 65–85.
- Rietbroek, R., Brunnabend, S.-E., Kusche, J., Schröter, J. & Dahle, C., 2016. Revisiting the contemporary sea-level budget on global and regional scales, *Proc. Natl. Acad. Sci. USA*, **113**(6), 1504–1509.
- Sun, Y., Riva, R. & Ditmar, P., 2016. Optimizing estimates of annual variations and trends in geocenter motion and  $J_2$  from a combination of GRACE data and geophysical models, *J. geophys. Res.*, **121**, 8352–8370.
- Swenson, S., Chambers, D. & Wahr, J., 2008. Estimating geocenter variations from a combination of GRACE and ocean model output, *J. geophys. Res.*, **113**(B8), B08410, doi:10.1029/2007JB005338.
- Trupin, A.S., Meier, M.F. & Wahr, J.M., 1992. Effects of melting glaciers on the Earth's rotation and gravitational field: 1965–1984, *Geophys. J. Int.*, **108**, 1–15.
- Wahr, J.M., Molenaar, M. & Bryan, F., 1998. Time variability of the Earth's gravity field: hydrological and oceanic effects and their possible detection using GRACE, *J. geophys. Res.*, **103**, 30 205–30 229.
- Wu, X., Heflin, M.B., Ivins, E.R. & Fukumori, I., 2006. Seasonal and interannual global surface mass variations from multisatellite geodetic data, *J. geophys. Res.*, **111**(B9), B09401, doi:10.1029/2005JB004100.
- Wu, X., Ray, J. & van Dam, T., 2012. Geocenter motion and its geodetic and geophysical implications, *J. Geodyn.*, **58**, 44–61.
- Wu, X. *et al.*, 2015. KALREF—A Kalman filter and time series approach to the International Terrestrial Reference Frame realization, *J. geophys. Res.*, **120**, 3775–3802.